Role of Dimensionality and Size in Governing the Drag Seebeck Coefficient of Doped Silicon Nanostructures: A Fundamental Understanding

Raja Sen, Nathalie Vast, Jelena Sjakste

Role of Dimensionality and Size in Governing the Drag Seebeck Coefficient of Doped Silicon Nanostructures: A Fundamental Understanding

Raja Sen,* Nathalie Vast, and Jelena Sjakste†
Laboratoire des Solides Irradies, CEA/DRF/IRAMIS, Ecole Polytechnique, CNRS, Institut Polytechnique de Paris, 91120 Palaiseau, France

In this theoretical study, we examine the influence of dimensionality, size reduction, and heat-transport direction on the phonon-drag contribution to the Seebeck coefficient of silicon nanostructures. Phonon-drag contribution arises from the momentum transfer between out-of-equilibrium phonon populations and charge carriers, and significantly enhances the thermoelectric coefficient. Our implementation of the phonon drag term accounts for the anisotropy of nanostructures such as thin films and nanowires through the boundary- and momentum-resolved phonon lifetime. Our approach also takes into acconout the spin-orbit coupling, which turns out to be crucial for hole transport. We reliably quantify the phonon drag contribution at various doping levels, temperatures, and nanostructure geometries for both electrons and holes in silicon nanstructures. Our results support the recent experimental findings, showing that a part of phonon drag contribution survives in 100 nm silicon nanostructures.

The nanostructuring of semiconductors provides a viable route to enhance the thermoelectric efficiency as compared to that of the bulk by tuning the transport properties [1–3]. Together with electrical and lattice thermal conductivity, the Seebeck coefficient - that links the electrical current to the temperature gradient - is a key physical quantity characterizing the performance of thermoelectric materials. For a nondegenerate semiconductor, there are two contributions to the total Seebeck coefficient ($S^{\rm tot}$): the diffusive ($S^{\rm diff}$) and the phonon drag ($S^{\rm drag}$) contributions. While the former comes from the diffusion of charge carriers under a temperature gradient, the latter arises from the momentum transfer between the out-of-equilibrium phonon populations and the charge carriers [4–8]. Despite the impossibility to separately measure the $S^{\rm diff}$ and $S^{\rm drag}$ contributions, the important role played by the phonon drag has been recognized experimentally by the strong increase of $S^{\rm tot}$ at low temperatures in semiconductors, where anharmonicity is reduced and out-of-equilibrium phonon populations are very large [9–14].

The individual contributions to $S^{\rm tot}$ can, however, be quantified theoretically by means of models with effective parameters [5, 15, 16] or by *ab initio* calculations [17–21]. For example, it has been recently shown by density functional theory (DFT) that at 300 K and low electron doping (10^{14} cm^{-3}), more than 30% of $S^{\rm tot}$ in silicon comes from $S^{\rm drag}$. Moreover, the relative contribution of $S^{\rm drag}$ with respect to $S^{\rm tot}$ increases even further at higher doping (and fixed temperature) or at (fixed doping and) temperatures lower than 300 K [17–21]. Nevertheless, downsizing a semiconductor to the sub-micron scale is expected to drastically reduce the mean free path (MFP) of phonons and in consequence, the drag contribution to $S^{\rm tot}$. Therefore, the Seebeck coefficient is expected to decrease monotonically with decreasing the size of the nanostructure [9–11, 13].

In spite of the great effort invested in studying the effect of nanostructuring on $S^{\rm tot}$ [22–26], no consensus has been reached about the role of $S^{\rm drag}$ at the nanoscale, even in the case of silicon [17, 27–31]. Indeed, from the theoretical side, Zhou *et al.* [17] have pointed out that phonons contributing to $S^{\rm drag}$ have longer MFPs than those contributing to the lattice thermal conductivity of Si. A consequence is that $S^{\rm drag}$ is expected to be strongly suppressed at 1 μm by the effect of size reduction [17]. In addition, in the experimental study of $S^{\rm tot}$, Sadhu *et al.* [27] have concluded that the $S^{\rm drag}$ component vanishes completely in Si nanowires having a characteristic length smaller than 100 nm. However, these studies contradict the findings of other experimental works which have suggested that the drag contribution in Si ultrathin films [28], nanowires [29, 30], and nanoribbons [31] does not vanish. The situation is further complicated by the possible presence of various competing effects on the nanoscale, such as the energy filtering effect induced by defects, which can lead to an increase of the total Seebeck coefficient [32–34]. Thus, to disentangle the intricate effects that govern the magnitude of $S^{\rm tot}$ on the nanoscale, a detailed understanding of the dependence of $S^{\rm drag}$ on the dimensionality and size of nanostructures is necessary and this can only be achieved through theory.

In this paper, we report the results of the systematic investigation of the influence of both size reduction and dimensionality on the phonon drag Seebeck coefficient of electron- and hole-doped silicon, by solving the coupled linearized Boltzmann transport equation (BTE) for charged carriers and for phonons, in combination with a fully *ab initio* description of the carrier-phonon interaction [35–41]. The coupling of the BTEs enables us to include in particular the effect of the out-of-equilibrium phonon populations which arise in presence of the temperature gradient. At variance with previous ones, the computational approach implemented in this work allows to account for the anisotropy of phonon

* rajasenphysics@gmail.com
† jelena.sjakste@polytechnique.edu

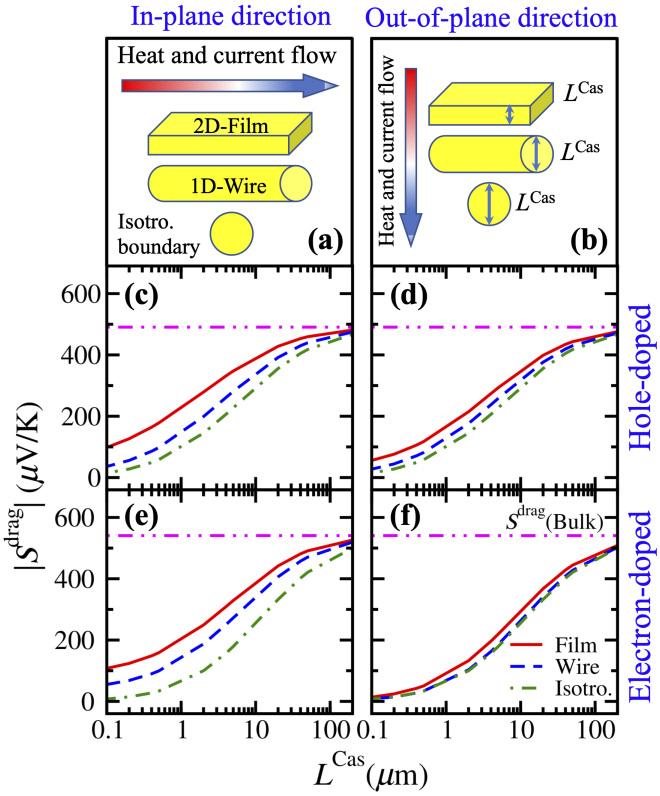

Figure 1. Panel a (b): Schema of the in-plane (out-of-plane) direction of heat and current flows as a function of the nanostructure dimensionality: 2D-Film, 1D-wire, and the isotropic boundary. Panel c (e): Variation of hole (electron) phonon drag Seebeck coefficient as a function of the Casimir length (L^{Cas}) in the in-plane direction at 300 K and 10^{14} cm^{-3} doping concentrations. Panel d (f): Same as panel c (e) in the out-of-plane direction.

scattering by nanostructure boundaries in the calculations of phonon drag Seebeck coefficient. In our work, the role of anisotropy and dimensionality of boundary scattering has been studied by considering two-dimensional (2D) nanofilms and one-dimensional (1D) nanowires, as well as isotropic boundaries (Fig. 1, panel a). The direction-resolved out-of-equilibrium phonon populations have been determined as a function of the nanostructure size, with the aim of quantifying the effect of the transport-direction-dependent phonon-boundary scattering in the phonon drag contribution. Moreover we have included the effect of spin-orbit coupling on the S^{tot} for holes, an effect which has been neglected so far for the Seebeck coefficient.

The electrical and heat currents produced by a temperature gradient experience a mutual drag via the interaction between charge carriers and phonons. This means that, in principle, the carrier-phonon scattering terms that govern the BTE for charge carriers and sometimes play a role in the BTE for phonons, depend both on the charge-carrier out-of-equilibrium distribution functions, $f_{\mathrm{n}\mathbf{k}}$, and on the out-of-equilibrium phonon populations $n_{\mathbf{q}\nu}$, where n, $\mathbf{k}$, ν, $\mathbf{q}$ are respectively the electronic band index, wave vector, phonon mode index, and wave vector. However, the electron-phonon scattering terms in the phonon BTE has proven necessary only close to the degenerate semiconductor limit, e.g., for carrier concentrations larger than 10^{19} cm^{-3} at 300 K in silicon [17]. In that case, a partial decoupling scheme [6, 7] can be used, in which the electron-phonon scattering terms in the phonon BTE are made dependent on the (equilibrium) Fermi-Dirac distribution function $f^0_{\mathrm{n}\mathbf{k}}$ [17, 19–21]. For low to moderate doping concentrations which do not exceed 10^{19} cm^{-3}, the effect of electron-phonon scattering on the phonon populations can be safely neglected [15, 18, 42]. In the present study, we follow the latter approximation and obtain the Seebeck coefficient of silicon nanostructures, including the phonon drag mechanism, by solving the charge-carrier BTE in the relaxation time approximation:

$$-\frac{\partial f^0_{\mathrm{n}\mathbf{k}}}{\partial \varepsilon_{\mathrm{n}\mathbf{k}}}\mathbf{v}_{\mathrm{n}\mathbf{k}}\cdot\left[\mathbf{E}e+\frac{\nabla_{\mathbf{r}}T}{T}\left(\varepsilon_{\mathrm{n}\mathbf{k}}-\mu\right)\right] -D^{\mathrm{drag}}_{\mathrm{n}\mathbf{k}}\left(g,\delta n\right)=-\left(\frac{\partial f_{\mathrm{n}\mathbf{k}}}{\partial t}\right)_{coll} \quad (1)$$

where $\mathbf{E}$ and $\nabla_{\mathbf{r}}T$ denote a small electric field and the temperature gradient, μ is the chemical potential for holes (electrons), $\mathbf{v}_{\mathrm{n}\mathbf{k}}$ and $\varepsilon_{\mathrm{n}\mathbf{k}}$ are respectively the charge-carrier group velocity and energy. The term $\left(\frac{\partial f_{\mathrm{n}\mathbf{k}}}{\partial t}\right)_{coll}$ includes all of the collisions associated with carrier-phonon and carrier-impurity scatterings.

The term $D^{\mathrm{drag}}_{\mathrm{n}\mathbf{k}}\left(g,\delta n\right)$ is the key quantity that describes the phonon drag mechanism, and can be written as [18, 42]:

$$\begin{aligned}D^{\mathrm{drag}}_{\mathrm{n}\mathbf{k}}\left(g,\delta n\right)=&\frac{2\pi}{\hbar}\sum_{\mathrm{m}\nu}\int\frac{d\mathbf{q}}{\Omega_{\mathrm{BZ}}}\left|g_{\mathrm{mn}\nu}\left(\mathbf{k},\mathbf{q}\right)\right|^2\\ &\times\{\delta n_{\mathbf{q}\nu}\delta\left(\varepsilon_{\mathrm{n}\mathbf{k}}-\varepsilon_{\mathrm{m}\mathbf{k}+\mathbf{q}}+\hbar\omega_{\mathbf{q}\nu}\right)\\ &+\delta n_{-\mathbf{q}\nu}\delta\left(\varepsilon_{\mathrm{n}\mathbf{k}}-\varepsilon_{\mathrm{m}\mathbf{k}-\mathbf{q}}-\hbar\omega_{-\mathbf{q}\nu}\right)\}\\ &\times\left(f^0_{\mathrm{m}\mathbf{k}+\mathbf{q}}-f^0_{\mathrm{n}\mathbf{k}}\right)\end{aligned} \quad (2)$$

where $g_{\mathrm{mn}\nu}\left(\mathbf{k},\mathbf{q}\right)$ is the carrier-phonon interaction matrix element and Ω_{BZ} is the volume of the first Brillouin zone (BZ). The (linearized) out-of-equilibrium phonon populations, $\delta n_{\mathbf{q}\nu}=n_{\mathbf{q}\nu}-n^0_{\mathbf{q}\nu}$, are expressed as:

$$\delta n_{\mathbf{q}\nu}=-\tau_{\mathbf{q}\nu}\frac{\nabla_{\mathbf{r}}T\cdot\mathbf{c}_{\mathbf{q}\nu}}{k_BT^2}\hbar\omega_{\mathbf{q}\nu}n^0_{\mathbf{q}\nu}\left(1+n^0_{\mathbf{q}\nu}\right) \quad (3)$$

and have been obtained by solving the phonon BTE in the single mode approximation with the D3Q code [43, 44]. Here, $\mathbf{c}_{\mathbf{q}\nu}$, $\tau_{\mathbf{q}\nu}$, $\omega_{\mathbf{q}\nu}$, and $n^0_{\mathbf{q}\nu}$ are respectively the group velocity, lifetime, frequency, and the (equilibrium) Bose-Einstein phonon populations. We have used our in-house modified version of the Electron-Phonon Wannier (EPW) code [45] to solve Eq. 1 (see Supplemental Materials).

Eqs. 1 and 2 give rise to an electrical current in the same direction as the heat flow (Fig. 1, panels a and b). Indeed, although expressed in a form similar to standard electron-phonon scattering processes, the term $D^{\rm drag}_{\rm n\mathbf{k}}(g,\delta n)$ is not a resistive process and contributes to the enhancement of the electrical current in the direction of the heat flow. We obtain the diffusion contribution when $\delta n_{\mathbf{q}\nu}=0$, and thereby calculate $S^{\rm drag}$ as $S^{\rm tot}|_{\delta n_{\mathbf{q}\nu}\neq 0}-S^{\rm diff}$.

In addition to the phonon-phonon and isotope scattering rates [43, 44], the inverse of the phonon lifetime $(\tau_{\mathbf{q}\nu})^{-1}$ is also determined by the phonon-boundary scattering rate which, for nanostructures, is the crucial quantity that controls the magnitude of $D^{\rm drag}_{\rm n\mathbf{k}}$. We have used the phonon momentum-resolved Casimir model to determine the transport-direction-dependent phonon-boundary scattering in nanostructures. The Casimir scattering rate for a phonon is given by [30, 46]:

$$(\tau^{\rm bound}_{\mathbf{q}\nu})^{-1}=\left(\frac{1-p}{1+p}\right)\frac{|\mathbf{c}^{\rm proj}_{\mathbf{q}\nu}|}{L^{\rm Cas}} \qquad (4)$$

where the Casimir scattering length, $L^{\rm Cas}$, represents the nanostructure size (Fig. 1, panels a and b). The specularity, p, ranges from 0 to 1 for completely diffusive to completely specular scattering, respectively. The velocity, $|\mathbf{c}^{\rm proj}_{\mathbf{q}\nu}|$, is the phonon group velocity $\mathbf{c}_{\mathbf{q}\nu}$ projected on the direction(s) in which the phonon transport is limited by the boundaries (see Supplemental Materials). It should be mentioned that while the anisotropy of the boundary scattering has been taken into account in several theoretical studies of lattice thermal conductivity [46–49], only the isotropic boundary (Fig. 1, panel a) has been considered so far in the studies of the phonon drag effect [30, 50]. The case of anisotropic phonon-boundary scattering presents a computational challenge, due to the reduced symmetry of the term $D^{\rm drag}_{\rm n\mathbf{k}}(g,\delta n)$ of Eq. 2 in presence of the anisotropic phonon lifetime $\tau_{\mathbf{q}\nu}$. This challenge can be overcome by performing the calculation of $D^{\rm drag}_{\rm n\mathbf{k}}(g,\delta n)$ without making use of crystal symmetry considerations and employing an additional $\mathbf{q}$-points filtering scheme (see Supplemental Materials).

We start by examining the effect of spin-orbit coupling (SOC) on the Seebeck coefficient for holes, as no such report is available in the literature. Our results for $S^{\rm tot}$ in hole-doped bulk silicon with and without SOC, together with the corresponding contributions from the diffusion and drag parts, are shown in Fig. 2 (panels a and b) as a function of carrier concentration at 300 K. Taking SOC into account leads to a decrease of $S^{\rm tot}$ at all concentrations, significantly improving the agreement with the available experimental data [11]. Turning now to the analysis of $S^{\rm diff}$ and $S^{\rm drag}$ contributions, the absolute value of $S^{\rm diff}$ (dashed line), as expected, decreases linearly with the increase of carrier doping [17–21], and is not affected by the presence/absence of SOC. In wide contrast, $S^{\rm drag}$ (dot-dashed line) remains nearly independent of the carrier concentration and is found to be

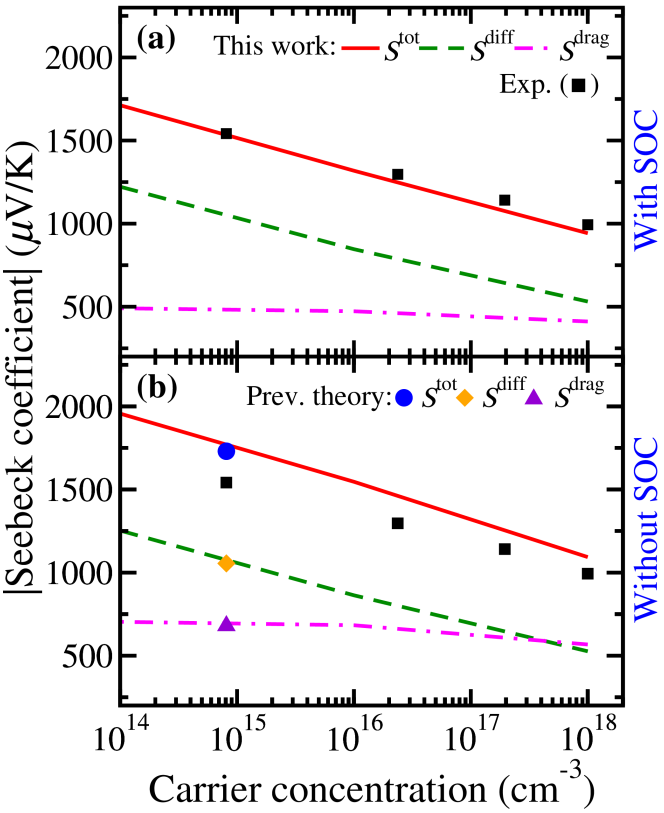

Figure 2. Calculated Seebeck coefficient of hole-doped bulk silicon (a) with and (b) without SOC interaction as a function of the carrier concentration at 300 K. Solid line: $S^{\rm tot}$, Dashed line: $S^{\rm diff}$, and Dot-dashed line: $S^{\rm drag}$. The circle, diamond, and triangle respectively denote the theoretical value of $S^{\rm tot}$, $S^{\rm diff}$, and $S^{\rm drag}$ taken from Ref. [17]. Squares: Experimental data [11].

strongly affected by SOC. Indeed, we find that the $S^{\rm drag}$ contribution is reduced by 30% when SOC interaction is accounted for. This reduction can be explained by the change of the band structure around the top of the valence band (VB) induced by SOC [51], which, in turn, affects the number of allowed electron-phonon interactions contributing to the phonon drag (the Dirac distribution in Eq. 2). Indeed, Poncé *et al.* [51] pointed out the improvement of the calculated hole effective masses in the valence band of silicon with SOC. We show that this is crucial also for the drag Seebeck coefficient for holes.

We now turn to the role of dimensionality, size, and direction in governing the drag Seebeck coefficient of silicon nanostructures. Our theoretical results (Fig. 1) show the effect of size reduction on $S^{\rm drag}$ for monocrystalline intrinsic samples of different geometries at 300 K. These results have been obtained for $p=0$ in Eq. 4 (completely diffusive boundary) and thus, should be regarded as the lowest threshold value of $S^{\rm drag}$. Our calculations show that $S^{\rm drag}$ is almost size-independent down to $L^{\rm Cas}\sim 100$ μm, and then decreases monotonically with the decrease in $L^{\rm Cas}$ for all dimensionalities and

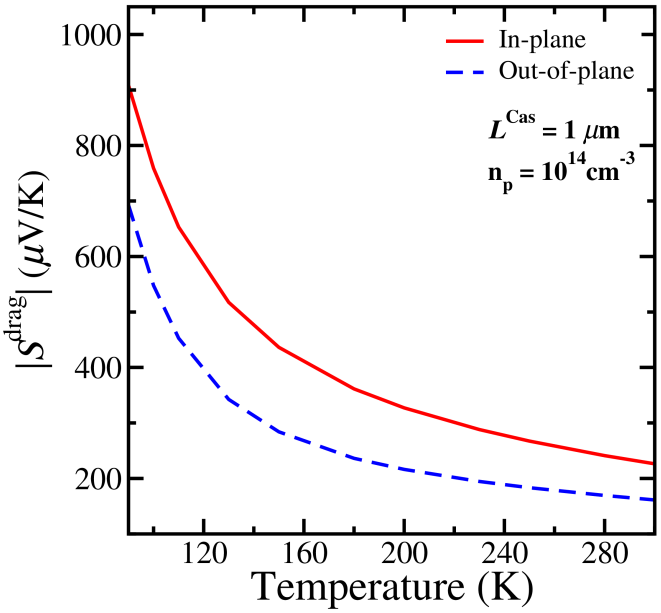

Figure 3. Variation of hole-phonon drag Seebeck coefficient of silicon thin film (with $L^{\rm Cas} = 1$ μm and doping 10^{14} cm^{-3}) as a function of temperature. The solid and dashed lines represent $S^{\rm drag}$ along the in-plane and out-of-plane directions of the thin film, respectively.

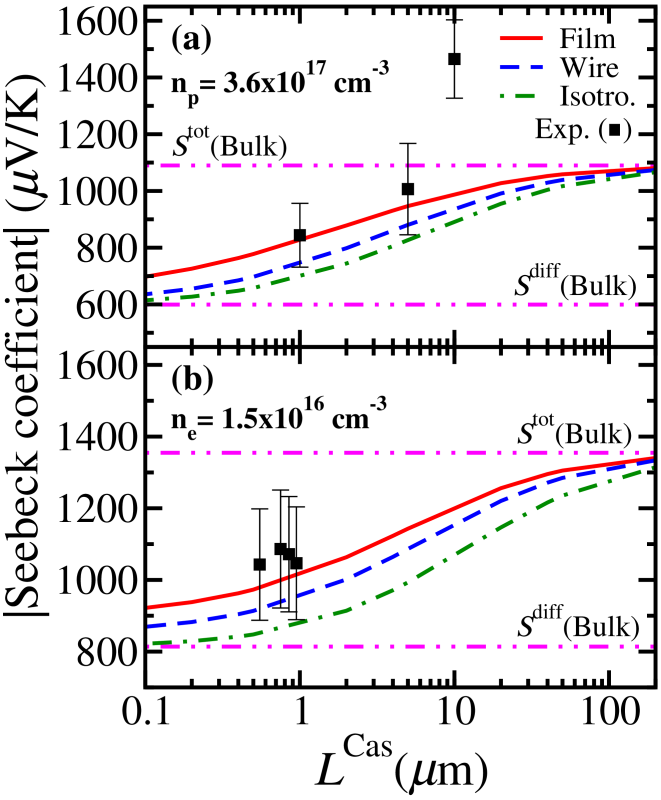

Figure 4. Variation of the total Seebeck coefficient ($S^{\rm tot}$) of (a) hole-doped (3.6×10^{17} cm^{-3}) and (b) electron-doped (1.5×10^{16} cm^{-3}) silicon nanowires as a function of the diameter ($L^{\rm Cas}$) at 300 K. Squares: Experimental data from Ref. [30] for holes and Ref. [33] for electrons.

heat transport directions.

However, one can observe a different rate of decrease of $S^{\rm drag}$ for in- and out-of-plane directions. For both hole- and electron-phonon drag effects, $S^{\rm drag}$ along the out-of-plane direction of thin films and nanowires behaves as in the case of the isotropic boundary, and is quenched almost completely as $L^{\rm Cas}$ approaches ~ 100 nm. At the same time, $S^{\rm drag}$ decreases at a slower rate along the in-plane direction of thin films and nanowires than in the out-of-plane one, reflecting the fact that the phonons are scattered less frequently by boundaries when traveling in the in-plane direction. Our study shows that for both low hole and electron doping, a silicon thin film (nanowire) of thickness (diameter) 100 nm can still preserve more than 20% (10%) of the bulk $S^{\rm drag}$ when measured along the in-plane direction.

Turning to the comparison with previous work, our results do not entirely confirm the conclusions of Ref. [27], in which the phonon drag Seebeck coefficient is reported to be quenched completely in silicon nanowires of diameter smaller that 100 nm. Rather, our results are found to be compatible with Refs. [30, 33], in which it has been found that a part of $S^{\rm drag}$ survives in nanostructures. One must note here that the remaining drag contribution which we predict for silicon nanostructures with $L^{\rm Cas} = 100$ nm would be within the error bar of the experimental measurements of Sadhu *et al.* [27] at moderate doping (3×10^{18} cm^{-3}).

We next predict the temperature dependence of $S^{\rm drag}$ in silicon nanostructures (Fig. 3). For hole-doped silicon thin film (10^{14} cm^{-3}) with $L^{\rm Cas} = 1$ μm, the $S^{\rm drag}$ contribution is found to grow with decreasing temperature. The in-plane temperature dependence is found similar to the out-of-plane one. This behaviour is consistent with the increase of $S^{\rm tot}$ of bulk silicon [11, 17] and is predicted here for the first time for the nanostructure.

Finally, in Fig. 4, we compare our theoretical results with recent experiments available in the literature: Ref. [30] for hole doped (panel a) and Ref. [33] for electron doped (panel b) silicon nanowires. These experiments were performed at room temperature and moderate doping concentrations (3.6×10^{17} cm^{-3} for hole doped and 1.5×10^{16} cm^{-3} for electron doped samples). As mentioned in the introduction, the nanostructuring can induce several competing effects on the experimentally measured Seebeck coefficient. Apart from a reduction of the drag effect, as discussed above, the energy filtering effect due to defects in the nanostructure can also play an important role. The latter effect leads to the increase of the Seebeck coefficient, even exceeding the bulk value. Although the study of the energy filtering effect is beyond the scope of our formalism, the comparison between our calculated results and experiments allows to gain insight into the relative role of different effects. Indeed, one can see in panel a of Fig. 4 that in agreement with our calculations, the experimentally measured hole

Seebeck coefficient in Ref. [30] was found to decrease with the decreasing nanostructure size, which is a clear indication that phonon drag contribution is still present for the nanostructure sizes under study. At the same time, some other effect, such as possibly the energy filtering effect due to defects, is clearly playing a role for the Seebeck coefficient measured in Ref. [30], which is demonstrated by the fact that the experimental Seebeck value at 10 μm exceeds the bulk value at the same doping concentration.

For the case of electrons [33], the Seebeck coefficients which were measured for defect-free nanowires with diameters 0.6-1 μm are found in good agreement with our calculated data, demonstrating the effectiveness of our theoretical scheme (Fig. 4, panel b). We note that the isotropic boundary model underestimates $S^{\rm tot}$ for both cases of electrons and holes.

In conclusion, in this work we have provided a detailed *ab initio* study of the effect of the dimensionality, size, and heat-transport direction on the phonon drag Seebeck coefficient in silicon nanostructures, accounting both for the anisotropy of the boundary scattering and for the spin-orbit coupling. Inclusion of the latter is shown to be mandatory to obtain a predictive description of the hole-phonon scattering. The implementation of the phonon drag term in combination with anisotropic scattering of phonons by nanostructure boundaries turns out to be crucial to evaluate the transport-direction-dependent out-of-equilibrium phonon populations in silicon nanostructures, and predict the phonon-drag contribution to the Seebeck coefficient. In particular, we have shown that even if phonon drag contribution is strongly reduced by nanostructuring, a silicon thin film (nanowire) of thickness (diameter) 100 nm can still preserve, at 300 K, more than 20% (10%) of the bulk $S^{\rm drag}$ when measured along the in-plane direction, for both electrons and holes. Our findings for silicon nanowires support the conclusion of the recent experimental work of Ref. [30] concerning the impact of phonon-boundary scattering on the hole Seebeck coefficient of silicon nanowires and show an excellent agreement with the electron Seebeck coefficient measured in Ref. [33]. At the same time, the remaining drag contribution which we predict for silicon nanostructures with $L^{\rm Cas} = 100$ nm would be within the error bar of the experimental measurements of Ref. [27] at moderate doping. Therefore, our results allow to resolve the apparent contradiction in previous litterature. Furthermore, we also predict that even if the remaining contribution of $S^{\rm drag}$ at 300 K is relatively small in silicon nanostructures, a remarkable increase of the phonon drag contribution is to be expected at low temperatures.

ACKNOWLEDGMENTS

Calculations have been performed with the Quantum ESPRESSO computational package [53], the EPW code [45], the D3Q code [43, 44] and the Wannier90 code [56]. This work has been granted access to HPC resources by he French HPC centers GENCI-IDRIS, GENCI-CINES and GENCI-TGCC (Project 2210) and by the Ecole Polytechnique through the 3L-HPC project. Financial supports from the ANR (PLACHO project ANR-21-CE50-0008, Macacqu flagship Labex Nanosaclay ANR-10-LABX-0035), from the DIM SIRTEQ, from the CNRS-CEA program "Basic reseach for energy" are gratefully acknowledged.

We acknowlege useful discussions with Dr. Natalio Mingo and Dr. Samuel Poncé, as well as the contribution of Dr. Gaston Kane on the preliminary stage of the project.

[1] J. He and T. Tritt, Science **357**, eaak9997 (2017).
[2] D. Dangić, S. Fahy, and I. Savić, Npj Comput. Mater. **6**, 195 (2020).
[3] L. Yang, D. Huh, R. Ning, V. Rapp, Y. Zeng, Y. Liu, S. Ju, Y. Tao, Y. Jiang, J. Beak, J. Leem, S. Kaur, H. Lee, X. Zheng, and R. Prasher, Nat. Commun. **12**, 3926 (2021).
[4] L. Gurevich, J. Phys. Moscow **9**, 477 (1945).
[5] C. Herring, Phys. Rev. **96**, 1163 (1954).
[6] D. Cantrell and P. Butcher, J. Phys. C: Solid State Phys. **20**, 1985 (1987).
[7] D. Cantrell and P. Butcher, J. Phys. C: Solid State Phys. **20**, 1993 (1987).
[8] Y. Gurevich and O. Mashkevich, Phys. Rep. **181**, 327 (1989).
[9] H. Frederikse, Phys. Rev. **92**, 248 (1953).
[10] T. Geballe and G. Hull, Phys. Rev. **94**, 1134 (1954).
[11] T. Geballe and G. Hull, Phys. Rev. **98**, 940 (1955).
[12] A. Bentien, S. Johnsen, G. Madsen, B. Iversen, and F. Steglich, Europhys. Lett. **80**, 17008 (2007).
[13] H. Takahashi, R. Okazaki, S. Ishiwata, H. Taniguchi, A. Okutani, M. Hagiwara, and I. Terasaki, Nat. Commun. **7**, 12732 (2016).
[14] A. Jaoui, G. Seyfarth, C. Rischau, S. Wiedmann, S. Benhabib, C. Proust, K. Behnia, and B. Fauqué, npj Quantum Mater. **5**, 94 (2020).
[15] G. D. Mahan, L. Lindsay, and D. A. Broido, J. Appl. Phys. **116**, 245102 (2014).
[16] M. Battiato, J. Tomczak, Z. Zhong, and K. Held, Phys. Rev. Lett. **114**, 236603 (2015).
[17] J. Zhou, B. Liao, B. Qiu, S. Huberman, K. Esfarjani, M. Dresselhaus, and G. Chen, Proc. Natl. Acad. Sci. U. S. A. **112**, 14777 (2015).
[18] M. Fiorentini and N. Bonini, Phys. Rev. B **94**, 085204 (2016).
[19] N. Protik and B. Kozinsky, Phys. Rev. B **102**, 245202 (2020).
[20] Q. Xu, J. Zhou, T. Liu, and G. Chen, Phys. Rev. Applied **16**, 064052 (2021).
[21] N. Protik, C. Li, M. Pruneda, D. Broido, and P. Ordejon,

npj Comput. Mater. **8**, 28 (2022).
[22] M. Pokharel, H. Zhao, K. Lukas, Z. Ren, C. Opeil, and B. Mihaila, MRS Commun. **3**, 31 (2013).
[23] G. Wang, L. Endicott, H. Chi, P. Lostak, and C. Uher, Phys. Rev. Lett. **111**, 046803 (2013).
[24] M. Kockert, D. Kojda, R. Mitdank, A. Mogilatenko, Z. Wang, J. Ruhhammer, M. Kroener, P. Woias, and S. Fischer, Sci. Rep. **9**, 20265 (2019).
[25] A. Nadtochiy, V. Kuryliuk, V. Strelchuk, O. Korotchenkov, P. Li, and S. Lee, Sci. Rep. **9**, 16335 (2019).
[26] M. Cabero, C. Guo, C. Wan, J. Hu, S. Liu, M. Zhao, L. Zhang, Q. Song, H. Wang, S. Tu, N. Li, L. Sheng, J. Chen, Y. Liu, B. Wei, J. Zhang, X. Han, H. Yu, and D. Yu, J. Phys. Chem. C **125**, 13167 (2021).
[27] J. Sadhu, H. Tian, J. Ma, B. Azeredo, J. Kim, K. Balasundaram, C. Zhang, X. Li, P. Ferreira, and S. Sinha, Nano Lett. **15**, 3159 (2015).
[28] F. Salleh, T. Oda, Y. Suzuki, Y. Kamakura, and H. Ikeda, Appl. Phys. Lett. **105**, 102104 (2014).
[29] A. Boukai, Y. Bunimovich, J. Tahir-Kheli, J. Yu, W. G. III, and J. Heath, Nature **451**, 168 (2008).
[30] K. Fauziah, Y. Suzuki, T. Nogita, Y. Kamakura, T. Watanabe, F. Salleh, and H. Ikeda, AIP Adv. **10**, 075015 (2020).
[31] H. Ryu, Z. Aksamija, D. Paskiewicz, S. Scott, M. Lagally, I. Knezevic, and M. Eriksson, Phys. Rev. Lett. **105**, 256601 (2010).
[32] J. Zide, D. Vashaee, Z. Bian, G. Zeng, J. Bowers, A. Shakouri, and A. Gossard, Phys. Rev. B **74**, 205335 (2006).
[33] N. S. Bennett, D. Byrne, and A. Cowley, Appl. Phys. Lett. **107**, 013903 (2015).
[34] Z. Liang, M. J. Boland, K. Butrouna, D. R. Strachan, and K. R. Graham, J. Mater. Chem. A **5**, 15891 (2017).
[35] F. Murphy-Armando and S. Fahy, Phys. Rev. Lett. **97**, 096606 (2006).
[36] M. Calandra, G. Profeta, and F. Mauri, Phys. Rev. B **82**, 165111 (2010).
[37] M. Bernardi, Eur. Phys. J. B **89**, 15 (2016).
[38] F. Giustino, Rev. Mod. Phys. **89**, 015003 (2017).
[39] J. Sjakste, K. Tanimura, G. Barbarino, L. Perfetti, and N. Vast, J. Phys.: Condens. Matter **30**, 353001 (2018).
[40] S. Poncé, W. Li, S. Reichardt, and F. Giustino, Rep. Prog. Phys. **83**, 036501 (2020).
[41] G. Brunin, H. P. C. Miranda, M. Giantomassi, M. Royo, M. Stengel, M. J. Verstraete, X. Gonze, G.-M. Rignanese, and G. Hautier, Phys. Rev. Lett. **125**, 136601 (2020).
[42] F. Macheda and N. Bonini, Phys. Rev. B **98**, 201201 (2018).
[43] L. Paulatto, F. Mauri, and M. Lazzeri, Phys. Rev. B **87**, 214303 (2013).
[44] G. Fugallo, M. Lazzeri, L. Paulatto, and F. Mauri, Phys. Rev. B **88**, 045430 (2013).
[45] S. Ponce, E. R. Margine, C. Verdi, and F. Giustino, Comp. Phys. Comm. **209**, 116 (2016).
[46] M. Markov, J. Sjakste, G. Fugallo, L. Paulatto, M. Lazzeri, F. Mauri, and N. Vast, Phys. Rev. B **93**, 064301 (2016).
[47] A. J. H. McGaughey, E. S. Landry, D. P. Sellan, and C. H. Amon, Appl. Phys. Lett. **99**, 131904 (2011).
[48] Y. Ma, Appl. Phys. Lett. **101**, 211905 (2012).
[49] C. Jeong, S. Datta, and M. Lundstrom, J. Appl. Phys. **111**, 093708 (2012).
[50] C. Li, N. Protik, P. Ordejon, and D. Broido, Mater. Today Phys. **27**, 100740 (2022).
[51] S. Poncé, E. Margine, and F. Giustino, Phys. Rev. B **97**, 121201 (2018).
[52] J. Leveillee, X. Zhang, E. Kioupakis, and F. Giustino, Phys. Rev. B (2023), accepted manuscript.
[53] P. Giannozzi, O. Andreussi, T. Brumme, O. Bunau, M. B. Nardelli, M. Calandra, R. Car, C. Cavazzoni, D. Ceresoli, M. Cococcioni, N. Colonna, I. Carnimeo, A. D. Corso, S. de Gironcoli, P. Delugas, R. A. D. J. A. Ferretti, A. Floris, G. Fratesi, G. Fugallo, R. Gebauer, U. Gerstmann, F. Giustino, T. Gorni, J. Jia, M. Kawamura, H.-Y. Ko, A. Kokalj, E. Küçükbenli, M. Lazzeri, M. Marsili, N. Marzari, F. Mauri, N. L. Nguyen, H.-V. Nguyen, A. O. de-la Roza, L. Paulatto, S. Poncé, D. Rocca, R. Sabatini, B. Santra, M. Schlipf, A. P. Seitsonen, A. Smogunov, I. Timrov, T. Thonhauser, P. Umari, N. Vast, X. Wu, and S. Baroni, J. Phys.: Condens. Matter **29**, 465901 (2017).
[54] J. P. Perdew and A. Zunger, Phys. Rev. B **23**, 5048 (1981).
[55] H. Monkhorst and J. Pack, Phys. Rev. B **13**, 5188 (1976).
[56] G. Pizzi, V. Vitale, R. Arita, S. Blugel, F. Freimuth, G. Géranton, M. Gibertini, D. Gresch, C. Johnson, T. Koretsune, J. Ibañez-Azpiroz, H. Lee, J. M. Lihm, D. Marchand, A. Marrazzo, Y. Mokrousov, J. I. Mustafa, Y. Nohara, Y. Nomura, L. Paulatto, S. Poncé, T. Ponweiser, J. Qiao, F. Thole, S. S. Tsirkin, M. Wierzbowska, N. Marzari, D. Vanderbilt, I. Souza, A. A. Mostofi, and J. R. Yates, J. Phys.: Condens. Matter **32**, 165902 (2020).
[57] R. Sen, N. Vast, and J. Sjakste, Appl. Phys. Lett. **120**, 082101 (2022).